Design and Synthesis of Pyrimidine-Based Iridium(III) Complexes with Horizontal Orientation for Orange and White Phosphorescent OLEDs

Lin-Song Cui, Yuan Liu, Xiang-Yang Liu, Zuo-Quan Jiang,* and Liang-Sheng Liao*

Jiangsu Key Laboratory for Carbon-Based Functional Materials & Devices, Institute of Functional Nano & Soft Materials (FUNSOM), Collaborative Innovation Center of Suzhou Nano Science and Technology, Soochow University, Suzhou, Jiangsu 215123, P.R. China

S *Supporting Information*

ABSTRACT: Two phosphorescent Ir(III) complexes Ir(ppm)$_2$(acac) and Ir-(dmppm)$_2$(acac) were synthesized and characterized with emission ranged at 584/600 nm and high photoluminescence quantum yields (PLQYs) of 0.90/0.92, respectively. The angle-dependent PL spectra analysis reveals that the two orange iridium(III) complexes embodied horizontal orientation property. The high photoluminescence quantum yield and high horizontal dipoles ratio determine their excellent device performance. The devices based on Ir(ppm)$_2$(acac) and Ir(dmppm)$_2$(acac) achieved efficiencies of 26.8% and 28.2%, respectively, which can be comparable to the best orange phosphorescent devices reported in the literature. Furthermore, with the introduction of FIrpic as sky-blue emitter, phosphorescent two-element white organic light-emitting devices (OLEDs) have been realized with external quantum efficiencies (EQEs) as high as 25%, which are the highest values among the reported two-element white OLEDs.

CIE (0.45, 0.41)
CT 2838 K
PE > 78.0 lm/W

CIE (0.448, 0.408)
CT 2856 K
PE < 10.0 lm/W

KEYWORDS: *organic light-emitting diodes, iridium complex, pyrimidine, orange emission, warm-white, horizontal orientation*
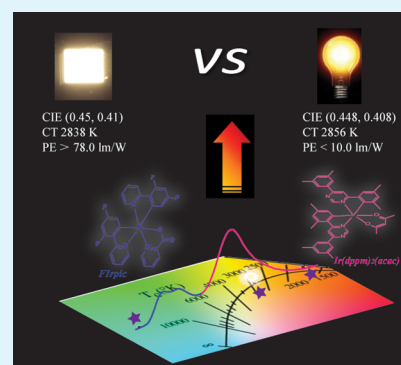
INTRODUCTION

Currently, ambient lighting applications consume ~20% of electricity power throughout the world; new technology such as organic light-emitting devices (OLEDs) with high electricity–light conversion efficiency have been considered, therefore, as one of the most promising solutions for reducing overall energy consumption.[1-3] How to employ all the electrically generated excitons is the key issue to achieve high efficiency in OLEDs.[4] According to spin statistics, 25% singlet (S) excitons and 75% triplet (T) excitons are generated under electrical excitation. However, 75% of the electrogenerated energy is dissipated as heat by triplet excitons in traditional fluorescence materials, leading to an internal quantum efficiency (IQE) less than 25%.[5] To increase the IQE of OLEDs, many efforts have been devoted to using the nonemissive triplet excitons to surpass the 25% IQE limitation of the OLEDs. In this regard, various kinds of phosphorescent light-emitting materials have been synthesized and studied to promote the lowest triplet excited state (T$_1$) to the ground state (S$_0$) transition (T$_1$ → S$_0$) for phosphorescence luminescence.[6-10] Among all the phosphors, iridium (IrIII) complexes remain the most effective materials because of their highly efficient emission properties, relatively short excited state lifetime, and good tunability in color.[11-18]

Recently, many research efforts have been made for high efficiency white OLEDs as they can be used for solid-state lighting (SSL), flat panel display (FPD), and backlight for liquid crystal display (LCD).[19-21] White emission can be composed of mixing three colors (red, green, and blue) or two colors (e.g., blue and orange). The three primary color strategy has its own advantage, especially in reaching the standard white light with CIE coordinates (0.33, 0.33).[22,23] Unfortunately, the three primary color strategy always suffer from the disadvantages of device complexity, high driving voltages, and undesired spectral variations.[24] However, from the viewpoint of lighting, white OLEDs tend to be designed to emit yellow–white emission, which is thereby considered as physiologically friendly illumination.[25] Typically, one important CIE coordinate (0.448, 0.408) with a color temperature (CT) of 2856 K is the so-called warm-white point. This chromaticity is observed in incandescent lamps, which are widely considered as the most comfortable artificial light sources for human perception.[26] For instance, Jou et al. demonstrated that the CT of light plays a vitally important role in human physiological health. Lights with high CT are suitable for illumination during the daytime, while low CT lights provide a more warm and comfortable sensation in the night.[25] Alternatively, the two complementary color strategies become a better option for fabrication of white OLEDs for lighting. Moreover, the emission spectra of the emitters should compensate to each other so that the whole visible region can be covered by this generated white spectrum.

Table 1. Physical Properties for the Iridium Complexes

complex	$\lambda_{abs}{}^a$ (nm)	$\lambda_{peak}{}^a$ (nm)	η^b (%)	$\tau_p{}^b$ (μs)	$k_r \times 10^{6b}$ (S^{-1})	$T_d/T_g{}^c$ (°C)	HOMO/LUMO^d (eV)
Ir(ppm)$_2$(acac)	271, 310, 387, 522	584	0.90	0.68	1.33	387/118	5.33/3.15
Ir(dmppm)$_2$(acac)	292, 433, 522	600	0.92	0.58	1.59	403/129	5.18/3.08

^{a}Measured in toluene solution (r. t.). ^{b}Measured in 8 wt % TCTA film. ^cT_d = decomposition temperature. T_g = glass transition temperature. ^{d}HOMO levels were measured by UPS; LUMO levels were calculated from HOMO and $E_g{}^{opt}$.

For blue phosphorescent emitters, a conventional choice is iridium(III) bis[(4,6-difluorophenyl)pyridinato-N,C2′]-picolinate (FIrpic), a sky-blue emitter with a central wavelength of 472 nm. However, most of the yellow or orange Ir(III) complexes show emission peaks around 560 nm, which are rather too short in wavelength to be complementary to the FIrpic phosphor. Therefore, due to the lack of appropriate orange phosphors, the performances of white OLEDs are still moderate and need to be further enhanced. To solve this problem, we focus on the design of C−N ligand for Ir(III) complexes, because the organic ligand is the determinant for the electroluminescence (EL) efficiency and the EL wavelength of the device.[27] Besides, some iridium(III) complexes have been reported to have preferred horizontal orientation property with improved EQEs over 30%.[28,29] Therefore, both the horizontal dipole ratio and the photoluminescence quantum yield of the emitting materials determine the device efficiency.

In this paper, two iridium(III) complexes based on diphenylpyrimidine ligand were successfully conceived and prepared. Additionally, the thermal stability, electrochemical properties, and photophysical behaviors associated with the two new complexes were carefully investigated. Interestingly, Ir(ppm)$_2$(acac) and Ir(dmppm)$_2$(acac) show high photoluminescence quantum yield (PLQY) and horizontally oriented ratio. The devices based on Ir(ppm)$_2$(acac) and Ir-(dmppm)$_2$(acac) achieved EQEs of 26.2% and 28.2%, respectively, which can be comparable to the best orange phosphorescent devices reported in the literature. Furthermore, Ir(dmppm)$_2$(acac) exhibited complementary wavelength to sky-blue emitting FIrpic for fabricating two-element white OLEDs (WOLEDs).[30] For example, at an optimal doping concentration of 1.0 wt % Ir(dmppm)$_2$(acac), the two-element white OLED exhibits incandescent lamp-like emission with an EQE of 28.6%. Besides, all devices show negligible efficiency roll-off. Thus, these excellent electroluminescent results demonstrate that pyrimidine-type ligands are efficient for iridium(III) complexes.

■ RESULTS AND DISCUSSION

Synthesis and Characterization. The key ligand-substituted pyrimidine and the Ir complexes were prepared by procedures described in Scheme S1 in the Supporting Information. The detailed synthetic routes and analyses are elucidated in the Supporting Information. Both Ir(ppm)$_2$(acac) and Ir(dmppm)$_2$(acac) were purified by temperature-gradient vacuum sublimation twice. Their chemical structures were well-characterized by ^{1}H NMR and ^{13}C NMR spectroscopies, time-of-flight (MALDI) mass spectrometry (MS), and elemental analysis.

Thermal Properties. The thermal properties of the compounds were evaluated by thermogravimetric analysis (TGA) and differential scanning calorimetry (DSC) under N$_2$ atmosphere with a heating rate of 10 °C per minute. The TGA and DSC data revealed that the two Ir complexes are thermally and morphologically stable materials as summarized in Table 1.

From the onset of the DSC curves (Figure 1), Ir(ppm)$_2$(acac) and Ir(dmppm)$_2$(acac) exhibited evident glass transition
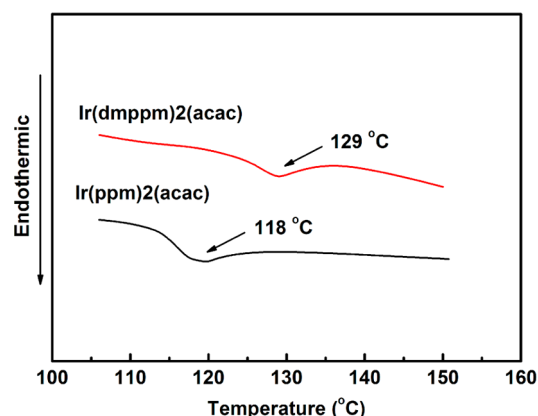

Figure 1. DSC curves of Ir complexes at a heating rate of 10 °C/min.

temperatures at 118 and 129 °C in the heating tests, respectively. On the other hand, Ir(ppm)$_2$(acac) and Ir-(dmppm)$_2$(acac) are thermally stable up to 387 and 403 °C, respectively, without degradation (see Figure S1 in the Supporting Information). These suggest that the two Ir complexes could form good quality thin films by vacuum deposition during device fabrication.

Optical Properties. Figure 2 depicts the optical absorption (UV−vis) and photoluminescence (PL) spectra of Ir-(ppm)$_2$(acac) and Ir(dmppm)$_2$(acac). The absorption spectra were recorded in toluene solutions at ambient temperature and showed similar trends. Comparatively, the UV absorption bands of Ir(dmppm)$_2$(acac) show a slight bathochromic shift. Their absorption spectra can be divided into three parts: the strong absorption bands ranging from 250−360 nm closely resemble those for the free ligand and thus they can be assigned to the spin-allowed ligand-centered $^1\pi-\pi^*$ intraligand charge-transfer transitions (^{1}ILCT); the absorption bands between 360 and 460 nm are assigned to spin-allowed metal-to-ligand charge transfer (S$_0 \rightarrow$ ^{1}MLCT) mixed with an interligand charge transfer (^{1}LLCT); and the weak absorption bands above 460 nm, which are likely ascribed to an admixture of the S$_0 \rightarrow$ ^{3}MLCT and $^3\pi-\pi^*$ excited states, stem from the strong spin−orbit coupling of the iridium complex. These couplings can also give rise to the ^{3}MLCT and $^3\pi-\pi^*$ bands. These features are similar to other complexes with (C−N)$_2$Ir(acac) molecular formula in previous reports.[31] On the basis of the absorption edges of Ir(ppm)$_2$(acac) and Ir(dmppm)$_2$(acac) at 588 and 595 nm, their corresponding optical energy gaps ($E_g{}^{opt}$) were estimated to be 2.10 and 2.08 eV, respectively.

The ambient temperature luminescence spectra of the two Ir complexes are reported in Figure 2. The Ir complexes Ir(ppm)$_2$(acac) and Ir(dmppm)$_2$(acac) emit strong phosphorescence at 584 and 600 nm, showing orange emissions. Iridium complex Ir(dmppm)$_2$(acac) with two extra methyl units on the
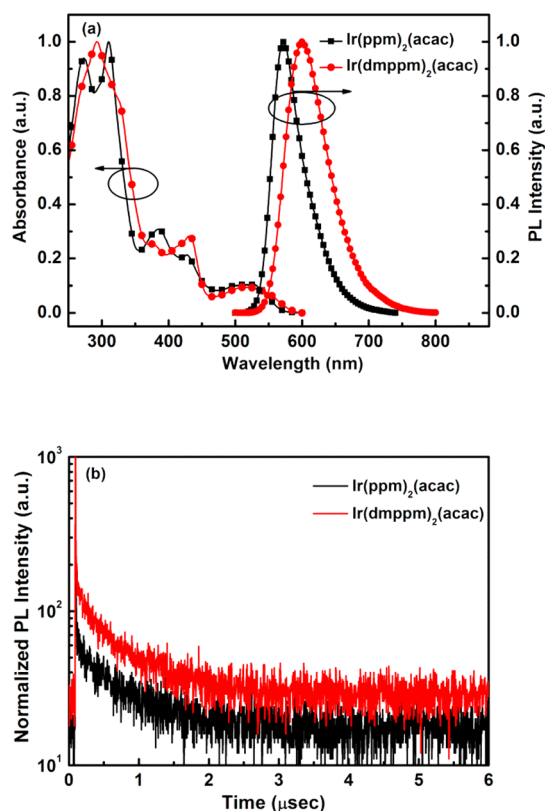
Figure 2. (a) Room-temperature UV−vis absorption and fluorescence (PL) spectra of Ir(ppm)$_2$(acac) and Ir(dmppm)$_2$(acac) in dilute degassed toluene solution. (b) Transient photoluminescence decay (excited at 420 nm) curves at room temperature for Ir(ppm)$_2$(acac) and Ir(dmppm)$_2$(acac) codeposited with TCTA.

phenyl is red-shifted by ∼26 nm relative to the iridium complex without the methyl substituent Ir(ppm)$_2$(acac). This fact implies that the electron-donating methyl group in benzene ring can efficiently promote the highest occupied molecular orbital (HOMO) energy level to decrease the energy gap between the HOMO and lowest unoccupied molecular orbital (LUMO) energy levels. Compared with the emission spectra at ambient temperature of the two Ir complexes, the PL spectra at 77 K (see Figure S2 in the Supporting Information) shows apparent vibrational fine structures, indicating that the mixing between the ^{3}MLCT and $^3\pi -\pi^*$ levels is so effective that almost ligand-centered emission could be observed in the frozen matrix.[32] All the spectroscopic data of Ir(ppm)$_2$(acac) and Ir(dmppm)$_2$(acac) are listed in Table 1.

The PLQYs (Φ_P) of Ir(ppm)$_2$(acac) and Ir(dmppm)$_2$(acac), which were dispersed in tris(4-carbazoyl-9-ylphenyl)amine (TCTA) (8 wt %) film, were measured as 0.90 and 0.92 at ambient temperature. These high Φ_P values can be attributed to the introduction of a pyrimidine unit into the molecules, which reduces the rate of radiationless deactivation. Such high Φ_P should be advantageous to fabricate highly efficient OLED devices. In addition, the emission lifetimes of Ir(ppm)$_2$(acac) and Ir(dmppm)$_2$(acac) dispersed in TCTA (8%) film at ambient temperature were also measured as 0.68 and 0.58 μs, respectively. Accordingly, the radiative lifetimes (τ_r) of the triplet excited state calculated from $\tau_r = \tau_p/\Phi_P$ are 0.75 and 0.63 μs, respectively. From the Φ_P and the τ_p values, assuming a unitary intersystem crossing efficiency, the radiative and the overall nonradiative rate constants (k_r and k_{nr}, respectively)

were calculated using the relationships $\Phi_P = \Phi_{ISC} \times (k_r/(k_r + k_{nr}))$ and $\tau_p = (k_r + k_{nr})^{-1}$. Here, Φ_{ISC} is the intersystem-crossing yield, which typically can be assumed to be 1.0 for iridium complexes with strong heavy-atom effect. Factually, no fluorescence could be observed for each compound at 293 or 77 K.[33,34] Complexes Ir(ppm)$_2$(acac) and Ir(dmppm)$_2$(acac) have similar k_r values, because they share the same core with slight difference at the appending small methyl group. As a result, it is found that the k_r values for Ir(ppm)$_2$(acac) and Ir(dmppm)$_2$(acac) are 1.33×10^6 s^{-1} and 1.59×10^6 s^{-1}, respectively. These high radiative rate constants would be beneficial for the highly efficient devices because the triplet excitons can decay rapidly through the radiative pathway. Additionally, the orientations of the transition dipole moments of Ir(ppm)$_2$(acac) and Ir(dmppm)$_2$(acac) in the TCTA films were determined by analyzing the angle-dependent PL spectra of the films. Figure S3 in the Supporting Information exhibits the measured angle-dependent PL intensities of the Ir-(ppm)$_2$(acac) and Ir(dmppm)$_2$(acac) from the 40 nm thick 8% TCTA film. The results fit the horizontal transition dipole ratios of 0.76 for Ir(ppm)$_2$(acac) and 0.78 for Ir-(dmppm)$_2$(acac). Thus, the high horizontal orientation ratios combined with high photoluminescence quantum yields of Ir(ppm)$_2$(acac) and Ir(dmppm)$_2$(acac) will determine their excellent performance in OLEDs.

Electrochemical Properties. To study the charge carrier injection properties of the complexes, the electrochemical behaviors of the Ir(ppm)$_2$(acac) and Ir(dmppm)$_2$(acac) were investigated by cyclic voltammetry (CV) using ferrocene as the reference, and the results are listed in Table 1. During the anodic scan in CH$_2$Cl$_2$ (Figure 3), the two complexes present
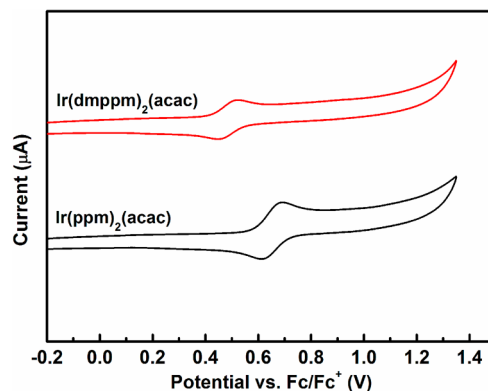

Figure 3. Cyclic voltammograms of Ir(ppm)$_2$(acac) and Ir-(dmppm)$_2$(acac) in dichloromethane solution for oxidation.

reversible oxidation peaks at 0.51 and 0.68 V, respectively. It is believed that this positive oxidation potential is attributed to the metal-centered Ir^{III}/Ir^{IV} oxidation couple, consistent with the previous reported Ir complexes.[35] On the other hand, the attachment of the electron-donating methyl groups to the phenyl ring produces a cathodic shift (∼0.17 eV) as compared to the unsubstituted one, which is consistent with the theoretical calculations (∼0.20 V), because the HOMO largely locates at the phenyl rings of the ligands. Therefore, Ir(dmppm)$_2$(acac) has a smaller band gap than that of Ir(ppm)$_2$(acac). From the oxidation potentials and the absorption edge data in UV spectra, the HOMO and LUMO energy levels of two complexes relative to the energy level of ferrocene (4.8 eV under vacuum) can be calculated. The

HOMO levels of Ir(ppm)$_2$(acac) and Ir(dmppm)$_2$(acac), also determined by using ultraviolet photospectroscopy (UPS, see Figures S4 and S5 in the Supporting Information) are 5.33 and 5.18 eV, respectively, which are consistent with the CV measurements. The results indicate that the generated excitons are able to be trapped on dopant in the doping system and lead to high device efficiency.[36]

Theoretical Calculations. To provide deeper insight into the photophysical properties, the triplet state geometries and triplet transition energies of the two orange Ir(III) complexes were calculated using time-dependent density functional theory (TD-DFT) calculations. The calculated T$_1$ → S$_0$ emission peaks were at 563 and 584 nm for Ir(ppm)$_2$(acac) and Ir(dmppm)$_2$(acac), respectively, which agree well with the phosphorescence peak wavelengths of the experimental results. This confirms the validity of the theoretical approach. According to the theoretical results, the T$_1$ states of Ir(ppm)$_2$(acac) and Ir(dmppm)$_2$(acac) mainly originate from HOMO → LUMO with a configuration interaction coefficient larger than 0.8. Figure 4 displays the HOMO and LUMO
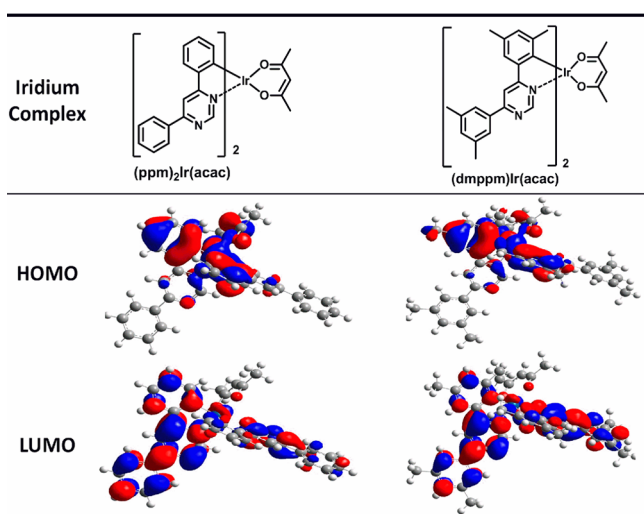

Figure 4. HOMO and LUMO surfaces of the two iridium complexes obtained from DFT calculations.

molecular orbitals of the two Ir complexes. The orbital distributions suggest that the HOMOs are composed of a mixture of Ir(III) d orbitals (t_{2g}) and phenyl π orbitals of the main ligand, while the LUMOs of the complexes are mainly located at the pyrimidine moiety and another phenyl group. Moreover, this electronic structure is significantly different from that of the commonly used green Ir complexes Ir(ppy)$_3$ or Ir(ppy)$_2$(acac), in which both the HOMO and the LUMO are distributed on the π orbitals of the 2-phenylpyridine ligands in addition to the Ir-d orbitals.[37] Therefore, the HOMOs and LUMOs of Ir(ppm)$_2$(acac) and Ir(dmppm)$_2$(acac) are located at different groups of the molecules. These evident HOMO/LUMO separations may be beneficial to efficient hole and electron−transporting properties, in which hole/electron can make intermolecular hopping via the respective transporting channels.[37] The S$_0$ and T$_1$ dipole moments were also calculated by DFT. The different transition dipole moments ($\Delta\mu$) between T$_1$ and S$_0$ are 3.46 and 3.52 debyes for Ir(ppm)$_2$(acac) and Ir(dmppm)$_2$(acac), respectively, which are higher than that of Ir(ppy)$_3$ (0.90 debye). According to the theory of the electronic transition, the k_r value is proportional to the square of the transition dipole moment.[38] Therefore, the larger $\Delta\mu$ may generate the fast radiative transitions of Ir(ppm)$_2$(acac) and Ir(dmppm)$_2$(acac). On the other hand, the transition dipole moment may also have some relation with the horizontal dipole ratio, which needs to be further investigated by additional research.

Electroluminescent Devices. The electroluminescent properties of Ir(ppm)$_2$(acac) and Ir(dmppm)$_2$(acac) were investigated because of the previously discussed promising properties. OLED devices with vacuum-sublimable orange iridium phosphors Ir(ppm)$_2$(acac) and Ir(dmppm)$_2$(acac) doped into the emissive layer were fabricated. Typical multilayer EL devices OA and OB were constructed using Ir(ppm)$_2$(acac) and Ir(dmppm)$_2$(acac) as emissive dopants with indium tin oxide (ITO) as the anode, 1,4,5,8,9,11-hexaazatriphenylene hexacarbonitrile (HAT-CN) as the hole-injection material, and 1,1-bis[4-[N,N-di(p-tolyl)amino]-phenyl]cyclohexane (TAPC) as the hole-transporting and electron-blocking material because of its suitable HOMO level of −5.5 eV for hole injection and high LUMO level of
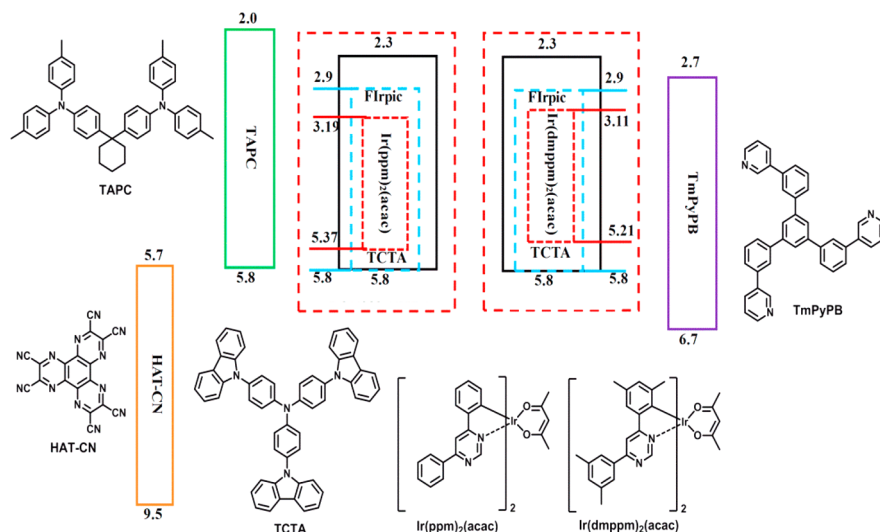

Figure 5. Energy levels of materials related to the devices.

−2.0 eV. Correspondingly, 1,3,5-tri[[(3-pyridyl)phen-3-yl]-benzene (TmPyPB) was used as the electron-transporting and hole-blocking material. Besides, due to the high triplet energies of TAPC (E_T = 2.87 eV) and TmPyPB (E_T = 2.78 eV), the generated triplet excitons could be effectively confined within the emitting layer.[39] Finally, 8-hydroxyquinolinolato-lithium (Liq) is the electron-injecting material and aluminum is the cathode of the device. The 4,4′,4″-tris(carbazol-9-yl)-triphenylamine (TCTA) was used as the triplet host material for the two Ir complexes due to its excellent performance as host for iridium complexes. The resultant orange phosphor-escent OLEDs (PHOLEDs) have a traditional configuration of ITO/HAT-CN (10 nm)/TAPC (45 nm)/TCTA:Ir-(ppm)$_2$(acac) or Ir(dmppm)$_2$(acac) (8 wt %, 20 nm)/TmPyPB (50 nm)/Liq (2 nm)/Al (120 nm) (Ir(ppm)$_2$(acac) = device OA; Ir(dmppm)$_2$(acac) = device OB). The two iridium complexes were used as the guest emitters with an optimized doping level at 8 wt %. Figure 5 shows the energy band diagrams and the molecular structures of the materials used in the fabricated monochromatic orange PHOLEDs. All the EL data are given in Table 2.

Table 2. Summary of Electroluminescence Data for OLEDs

device	V^a (v)	$\eta_{ext}{}^b$ (%)	CIE^c	CT^c (K)
OA	3.3	26.8, 23.0, 17.9	(0.50, 0.49)	2673
OB	3.2	28.2, 27.3, 24.5	(0.57, 0.42)	1861
W1	3.0	28.3, 26.5, 23.1	(0.51, 0.43)	2151
W2	3.0	28.6, 26.6, 22.7	(0.45, 0.41)	2838
W3	3.0	25.1, 23.6, 21.0	(0.41, 0.42)	3585

^{a}Voltage (V) at 100 cd/m^2. ^{b}External quantum efficiency (η_{ext}) in the order of maximum, at 1000 and 5000 cd/m^2. ^{c}Recorded at 10 mA/cm^2.

Figure S6 in the Supporting Information depicts the EL spectra of device OA and device OB. The two Ir complexes show orange EL signals peaking at 584 and 596 nm, respectively, which matched well with the PL spectra in solution. The resemblances between the PL and EL spectra indicate the absence of aggregation or π−π stacking at these doping ratios. On the other hand, there are no undesirable emission peaks from TCTA, suggesting an effective energy transfer from the host exciton to the phosphor molecule in the emission layer. The current density−voltage−luminance (J−V−L) characteristics are provided in Figure S7 in the Supporting Information. Figure 6 shows the EQE, current efficiency (CE), and power efficiency (PE) versus luminescence characteristics of device OA and device OB.

Both devices exhibit efficient orange electroluminescence (EL) with turn-on voltages at 3.0 and 2.8 V for Ir(ppm)$_2$(acac) and Ir(dmppm)$_2$(acac), respectively. The peak EQE, PE, and CE were 26.8%, 72.3 lm/W, and 77.0 cd/A for device OA at a bias of 3.3 V, and 28.2%, 61.2 lm/W, and 66.0 cd/A for device OB at a bias of 3.2 V. Generally, efficiency roll-off at high current is due to the combination of triplet−triplet annihilation and field-induced quenching effects.[40] Gratifyingly, the efficiency decrease is not obvious while the efficiency of OB is quite stable at the benchmark luminance of 5000 cd/m^2, and the EQE of device OB remained at 24.5%. Such a good performance can be attributed to the relatively short emission lifetimes of the Ir(dmppm)$_2$(acac). To our knowledge, the performances of the present orange light-emitting devices are among the best reported results.
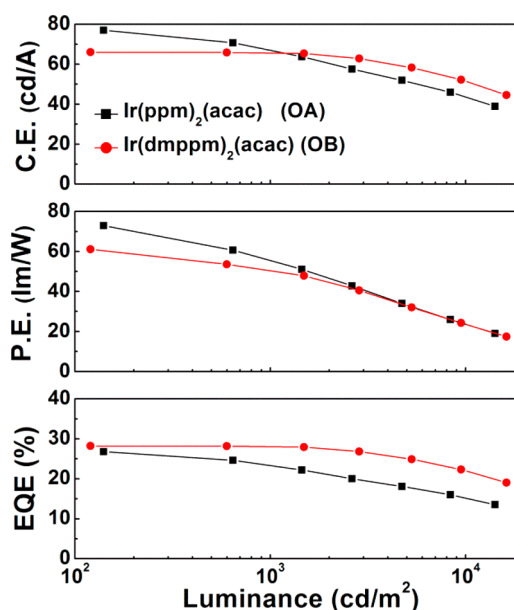

Figure 6. EQE, PE, and CE versus luminescence of devices OA and OB.

In addition, the stability of device OB is evaluated, and its half lifetime (T_{50}) is shown in Figure S8 in the Supporting Information. Device OB with Ir(dmppm)$_2$(acac) as phosphor material exhibited a longer half lifetime of 298 h, which is ∼2.6 times longer than that in the device using PO-01 as a phosphor material (115 h). This indicates that the pyrimidine-based Ir complexes show superiority in electroluminescence stability for OLEDs.

Generally, the development of orange light-emitting OLEDs with high performance is essential for constructing high-quality white OLEDs. On the other hand, the suitable CIE coordinates of device OB are effectively available to mix with the traditional sky-blue emitting FIrpic for fabricating two-element WOLEDs. Therefore, we employed Ir(dmppm)$_2$(acac) and FIrpic as the doped emitters to fabricate two-element white PHOLEDs with a similar configuration. The blue emission peak at ∼476 nm can be assigned to FIrpic, while the orange emission peak at ∼594 nm is due to Ir(ppm)$_2$(acac). To optimize EL efficiency and apparent color, devices with cascade doping levels were fabricated. The concentration of FIrpic was fixed as 10 wt %, while the doping concentration of Ir(dmppm)$_2$(acac) reduced from 1.5 to 0.5 wt % (devices W1−3). As the Ir-(dmppm)$_2$(acac) concentration increases, the intensity of the orange emission increases relatively, which is the result of more excitons being transferred to Ir(dmppm)$_2$(acac). All the EL data were collected in Table 2.

All three white devices show excellent performances, with EQEs exceeding 25%. Figure 7 illustrates their efficiency curves versus luminance and their emission characteristics. Device W1 with 1.5% doped Ir(dmppm)$_2$(acac) appears to give more orange emission than expected. The CIE coordinates lie in the yellow region, resulting in a yellowish-white light emission of W1 with CIE coordinates of (0.51, 0.43) and a correlated color temperature (CCT) of 2151 K. To make the CIE 1931 chromaticity coordinates approach (0.448, 0.408) for better warm-white standard illuminant, we reduce the doping rate of Ir(dmppm)$_2$(acac) to 1.0% and 0.5%, respectively. The emissions of W2 and W3 were adjusted to more desirable white light with CIE coordinates of (0.45, 0.41) and (0.41,
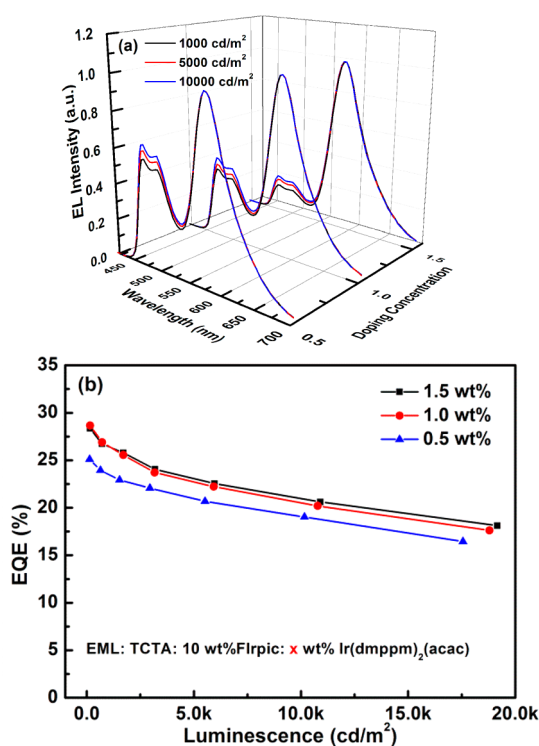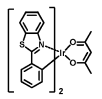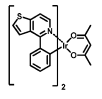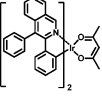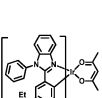
Figure 7. (a) Normalized EL spectra of device W1−3 at various luminescences. (b) External quantum efficiency versus luminescence of devices W1−3.

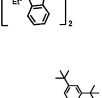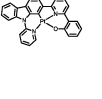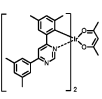0.42) and CTs of 2838 and 3585 K, respectively. No evident color variations at different brightnesses were observed for the two devices. Their CIE coordinates changed from (0.45, 0.41)/ (0.41, 0.42) at 1000 cd/m² to (0.44, 0.41)/(0.40, 0.42) at 10 000 cd/m², both of them shifting only by (0.01, 0.00). Device W2 showed an EQE of 28.6% and a PE of 78.0 lm/W, which greatly outnumbered the incandescent lamp (∼10 lm/ W) with similar CT. At a high brightness of 5000 cd/m², the EQE remains at 22.7% with a roll-off value of 21%. W3 also exhibits high efficiencies of 25.1% for the EQE with low-efficiency roll-offs. In addition, the driving voltages of W2 and W3 were <3.4 V (1000 cd/m²) and <4.5 V (5000 cd/m²), respectively. These low driving voltages, low-efficiency roll-offs, and higher color qualities could fulfill the requirements for lighting applications. Although the CRI of W1−3 (≈68) is not very high, as predicted for such two-color systems, it is still higher than sodium lamps and other reported two-element white WOLEDs. This improvement could be ascribed to the new orange Ir complex, especially the Ir(dmppm)₂(acac) with longer emission wavelength. It also could be envisaged that, by replacing the sky-blue component with a deep-blue component, the CRI can be further improved. Table 3 shows the EL efficacy and CIE parameters of our work as well as other two-element white OLEDs reported in the literature. It reveals that our current device efficiencies are among the best results of other two-element white OLEDs. Thus, this work represents a significant improvement toward the realization of commercial white lighting sources.

Table 3. Current State-of-the-Art Literature Data for Two-Element White OLEDs

Yellow Emitter	λ_{peak}(nm)	Active layers	EQE(%)	CIE	CT(K)	Ref.
	565	Host:FIrpic:Ir(bt)2(acac)	22.9	(0.39, 0.45)	4140	41
	560	PBCz:FIrpic:PO-01	24.6	(0.34, 0.47)	4943	26(b)
	578	CzSi:(fmoppy)₂Ir(tfpypz) /CBP:(dpiq)₂Ir(acac)	21.5	(0.44, 0.45)	3239	16
	570	p-POSiTPA:FIr6 /p-POSiTPA:(fbi)₂Ir(acac)	18.7	(0.42, 0.42)	3381	42
		p-BISiTPA:FIrpic/ p-BISiTPA:(fbi)₂Ir(acac)	19.1	(0.38, 0.44)	---	43
	553	TCTA:Y-Pt/mCP:FIrpic	16	(0.34, 0.44)	5352	44
	596	Host:FIrpic: 1.0% wt Ir(dmppm)₂(acac)	28.6	(0.45, 0.41)	3585	This work
		Host:FIrpic: 0.5% wt Ir(dmppm)₂(acac)	25.6	(0.41, 0.42)	2838	This work

CONCLUSIONS

In summary, we have successfully developed a new strategy for the preparation of phosphorescent iridium complexes by using pyrimidine-based ligands. Two new orange iridium complexes Ir(ppm)$_2$(acac) and Ir(dmppm)$_2$(acac) were synthesized and characterized with orange emission at 584/600 nm and high PLQYs of 0.90/0.92, respectively. The angle-dependent PL spectra analysis indicated that the two orange iridium(III) complexes showed a horizontal orientation property. The high photoluminescence quantum yield and horizontal dipoles ratio determine the excellent device performance and high efficiency. Orange OLEDs containing Ir(ppm)$_2$(acac) and Ir-(dmppm)$_2$(acac) as the dopants exhibited very high performance, with maximum EQEs of 26.8% and 28.2%, respectively, which can be comparable to the best orange phosphorescent devices reported in the literature. We also successfully utilized Ir(dmppm)$_2$(acac) incorporated into another sky-blue phosphor FIrpic to fabricate bicolor white OLED devices. Encouragingly, the white devices show high efficiencies as well as stable CIE. Particularly, WB2 shows incandescent lamp-like illuminant and achieves an EQE of 28.6%. These results indicate that there will be considerable scope for exploring new pyrimidine-based ligands to obtain highly efficient orange and even red Ir complexes.

ASSOCIATED CONTENT

Supporting Information

Synthetic details, characterization methods and spectra, TGA curves, low-temperature spectra, angle-dependent PL intensities, UPS spectra, EL spectra, $I-V-L$ curves of devices, current efficiency results, and device lifetime measurement. The Supporting Information is available free of charge on the ACS Publications website at DOI: 10.1021/acsami.5b02541.

AUTHOR INFORMATION

Corresponding Authors
*zqjiang@suda.edu.cn
*lsliao@suda.edu.cn

Notes
The authors declare no competing financial interest.

ACKNOWLEDGMENTS

REFERENCES

(1) Reineke, S.; Lindner, F.; Schwartz, G.; Seidler, N.; Walzer, K.; Lüssem, B.; Leo, K. White Organic Light-Emitting Diodes with Fluorescent Tube Efficiency. *Nature* **2009**, *459*, 234−238.

(2) Liao, L. S.; Slusarek, W. K.; Hatwar, T. K.; Ricks, M. L.; Comfort, D. L. Tandem Organic Light-Emitting Diode Using Hexaazatriphenylene Hexacarbonitrile in the Intermediate Connector. *Adv. Mater.* **2008**, *20*, 324−329.

(3) Wang, Q.; Ding, J.; Ma, D.; Cheng, Y.; Wang, L.; Jing, X.; Wang, F. Harvesting Excitons Via Two Parallel Channels for Efficient White Organic LEDs with Nearly 100% Internal Quantum Efficiency: Fabrication and Emission-Mechanism Analysis. *Adv. Funct. Mater.* **2009**, *19*, 84−95.

(4) Tang, C. W.; VanSlyke, S. A. Organic Electroluminescent Diodes. *Appl. Phys. Lett.* **1987**, *51*, 913−915.

(5) Sasabe, H.; Kido, J. Multifunctional Materials in High-Performance OLEDs: Challenges for Solid-State Lighting. *Chem. Mater.* **2010**, *23*, 621−630.

(6) Baldo, M. A.; O'Brien, D. F.; You, Y.; Shoustikov, A.; Sibley, S.; Thompson, M. E.; Forrest, S. R. Highly Efficient Phosphorescent Emission from Organic Electroluminescent Devices. *Nature* **1998**, *395*, 151−154.

(7) Fan, C.; Yang, C. Yellow/Orange Emissive Heavy-Metal Complexes as Phosphors in Monochromatic and White Organic Light-Emitting Devices. *Chem. Soc. Rev.* **2014**, *43*, 6439−6469.

(8) Chen, X. L.; Yu, R.; Zhang, Q. K.; Zhou, L. J.; Wu, X. Y.; Zhang, Q.; Lu, C. Z. Rational Design of Strongly Blue-Emitting Cuprous Complexes with Thermally Activated Delayed Fluorescence and Application in Solution-Processed OLEDs. *Chem. Mater.* **2013**, *25*, 3910−3920.

(9) Zhang, Q.; Komino, T.; Huang, S.; Matsunami, S.; Goushi, K.; Adachi, C. Triplet Exciton Confinement in Green Organic Light-Emitting Diodes Containing Luminescent Charge-Transfer Cu (I) Complexes. *Adv. Funct. Mater.* **2012**, *22*, 2327−2336.

(10) Chi, Y.; Chou, P. T. Contemporary Progresses on Neutral, Highly Emissive Os (II) and Ru (II) Complexes. *Chem. Soc. Rev.* **2007**, *36*, 1421−1431.

(11) Wang, R.; Liu, D.; Ren, H.; Zhang, T.; Yin, H.; Liu, G.; Li, J. Highly Efficient Orange and White Organic Light-Emitting Diodes Based on New Orange Iridium Complexes. *Adv. Mater.* **2011**, *23*, 2823−2827.

(12) Fan, C.; Li, Y.; Yang, C.; Wu, H.; Qin, J.; Cao, Y. Phosphoryl/Sulfonyl-Substituted Iridium Complexes as Blue Phosphorescent Emitters for Single-Layer Blue and White Organic Light-Emitting Diodes by Solution Process. *Chem. Mater.* **2012**, *24*, 4581−4587.

(13) Chou, H. H.; Li, Y. K.; Chen, Y. H.; Chang, C. C.; Liao, C. Y.; Cheng, C. H. New Iridium Dopants for White Phosphorescent Devices: Enhancement of Efficiency and Color Stability by an Energy-Harvesting Layer. *ACS Appl. Mater. Interfaces* **2013**, *5*, 6168−6175.

(14) Huang, W. S.; Lin, J. T.; Chien, C. H.; Tao, Y. T.; Sun, S. S.; Wen, Y. S. Highly Phosphorescent Bis-cyclometalated Iridium Complexes Containing Benzoimidazole-Based Ligands. *Chem. Mater.* **2004**, *16*, 2480−2488.

(15) Jou, J. H.; Lin, Y. X.; Peng, S. H.; Li, C. J.; Yang, Y. M.; Chin, C. L.; Hu, J. P. Highly Efficient Yellow Organic Light Emitting Diode with a Novel Wet- and Dry-Process Feasible Iridium Complex Emitter. *Adv. Funct. Mater.* **2014**, *24*, 555−562.

(16) Li, G.; Zhu, D.; Peng, T.; Liu, Y.; Wang, Y.; Bryce, M. R. Very High Efficiency Orange-Red Light-Emitting Devices with Low Roll-Off at High Luminance Based on an Ideal Host−Guest System Consisting of Two Novel Phosphorescent Iridium Complexes with Bipolar Transport. *Adv. Funct. Mater.* **2014**, *24*, 7420−7426.

(17) Cao, H.; Shan, G.; Wen, X.; Sun, H.; Su, Z.; Zhong, R.; Zhu, D. An Orange Iridium (III) Complex with Wide-Bandwidth in Electroluminescence for Fabrication of High-Quality White Organic Light-Emitting Diodes. *J. Mater. Chem. C* **2013**, *1*, 7371−7379.

(18) Zhou, G.; Wong, W. Y.; Yang, X. Focus Reviews. *Chem.—Asian J.* **2011**, *6*, 1706−1727.

(19) Li, G.; Fleetham, T.; Li, J. Efficient and Stable White Organic Light-Emitting Diodes Employing a Single Emitter. *Adv. Mater.* **2014**, *26*, 2931−2936.

(20) Sasabe, H.; Kido, J. Development of High Performance OLEDs for General Lighting. *J. Mater. Chem. C* **2011**, *1*, 1699−1707.

(21) Cui, L. S.; Dong, S. C.; Liu, Y.; Li, Q.; Jiang, Z. Q.; Liao, L. S. A Simple Systematic Design of Phenylcarbazole Derivatives for Host Materials to High-Efficiency Phosphorescent Organic Light-Emitting Diodes. *J. Mater. Chem. C* **2013**, *1*, 3967−3975.

(22) Hofmann, S.; Furno, M.; Lüssem, B.; Leo, K.; Gather, M. C. Investigation of Triplet Harvesting and Outcoupling Efficiency in Highly Efficient Two-Color Hybrid White Organic Light-Emitting Diodes. *Phys. Status Solidi A* **2013**, *210*, 1467−1475.

(23) Kamtekar, K. T.; Monkman, A. P.; Bryce, M. R. Recent Advances in White Organic Light-Emitting Materials and Devices (WOLEDs). *Adv. Mater.* **2010**, *22*, 572−582.

(24) Peng, T.; Yang, Y.; Bi, H.; Liu, Y.; Hou, Z.; Wang, Y.; Peng, T.; Yang, Y.; Bi, H.; Liu, Y.; Hou, Z.; Wang, Y. Highly Efficient White Organic Electroluminescence Device Based on a Phosphorescent Orange Material Doped in A Blue Host Emitter. *J. Mater. Chem.* **2011**, *21*, 3551−3553.

(25) Jou, J. H.; Hsieh, C. Y.; Tseng, J. R.; Peng, S. H.; Jou, Y. C.; Hong, J. H.; Lin, C. H. Candle Light-Style Organic Light-Emitting Diodes. *Adv. Funct. Mater.* **2013**, *23*, 2750−2757.

(26) Hu, Y.; Zhang, T.; Chen, J.; Ma, D.; Cheng, C. H. Hybrid Organic Light-Emitting Diodes with Low Color-Temperature and High Efficiency for Physiologically-Friendly Night Illumination. *Israel J. Chem.* **2014**, *54*, 979−985.

(27) Li, T. Y.; Liang, X.; Zhou, L.; Wu, C.; Zhang, S.; Liu, X.; Zuo, J. L. N-Heterocyclic Carbenes: Versatile Second Cyclometalated Ligands for Neutral Iridium(III) Heteroleptic Complexes. *Inorg. Chem.* **2015**, *54*, 161−173.

(28) Kim, K. H.; Moon, C. K.; Lee, J. H.; Kim, S. Y.; Kim, J. J. Highly Efficient Organic Light-Emitting Diodes with Phosphorescent Emitters Having High Quantum Yield and Horizontal Orientation of Transition Dipole Moments. *Adv. Mater.* **2014**, *26*, 3844−3847.

(29) Lee, S.; Shin, H.; Kim, J. J. High-Efficiency Orange and Tandem White Organic Light-Emitting Diodes Using Phosphorescent Dyes with Horizontally Oriented Emitting Dipoles. *Adv. Mater.* **2014**, *26*, 5864−5868.

(30) Sun, D.; Zhou, X.; Liu, J.; Sun, X.; Li, H.; Ren, Z.; Ma, D.; Bryce, M. R.; Yan, S. Solution-Processed Blue/Deep Blue and White Phosphorescent Organic Light-Emitting Diodes (PhOLEDs) Hosted by a Polysiloxane Derivative with Pendant mCP (1,3-bis(9-carbazolyl)-benzene). *ACS Appl. Mater. Interfaces* **2015**, DOI: 10.1021/am507592s.

(31) Yersin, H.; Rausch, A. F.; Czerwieniec, R.; Hofbeck, T.; Fischer, T. The Triplet State of Organo-Transition Metal Compounds. Triplet Harvesting and Singlet Harvesting for Efficient OLEDs. *Coord. Chem. Rev.* **2011**, *255*, 2622−2652.

(32) Chen, S.; Tan, G.; Wong, W.-Y.; Kwok, H.-S. White Organic Light-Emitting Diodes with Evenly Separated Red, Green, and Blue Colors for Efficiency/Color-Rendition Trade-Off Optimization. *Adv. Funct. Mater.* **2011**, *21*, 3785−3793.

(33) Wong, W. Y.; Zhou, G. J.; Yu, X. M.; Kwok, H. S.; Tang, B. Z. Amorphous Diphenylaminofluorene-Functionalized Iridium Complexes for High-Efficiency Electrophosphorescent Light-Emitting Diodes. *Adv. Funct. Mater.* **2006**, *16*, 838−846.

(34) Monti, F.; Kessler, F.; Delgado, M.; Frey, J.; Bazzanini, F.; Accorsi, G.; Armaroli, N.; Bolink, H. J.; Ortí, E.; Scopelliti, R.; Nazeeruddin, M. K.; Baranoff, E. Charged Bis-Cyclometalated Iridium(III) Complexes with Carbene-Based Ancillary Ligands. *Inorg. Chem.* **2013**, *52*, 10292−10305.

(35) Nazeeruddin, M. K.; Wegh, R. T.; Zhou, Z.; Klein, C.; Wang, Q.; Angelis, F. D.; Fantacci, S.; Gratzel, M. Efficient Green-Blue-Light-Emitting Cationic Iridium Complex for Light-Emitting Electrochemical Cells. *Inorg. Chem.* **2006**, *45*, 9245−9250.

(36) Wang, Z.-Q.; Xu, C.; Dong, X.-M.; Zhang, Y.-P.; Hao, X.-Q.; Gong, J.-F.; Song, M.-P.; Ji, B.-M. Synthesis, Structure and Properties of a Novel Iridium(III) Pyrimidine Complex. *Inorg. Chem. Commun.* **2011**, *14*, 316−319.

(37) Peng, T.; Li, G.; Ye, K.; Wang, C.; Zhao, S.; Liu, Y.; Hou, Z.; Wang, Y. Highly Efficient Phosphorescent OLEDs with Host-Independent and Concentration-Insensitive Properties Based on a Bipolar Iridium Complex. *J. Mater. Chem. C* **2013**, *1*, 2920−2926.

(38) Yersin, H.; Finkenzeller, W. J. Triplet Emitters for Organic Light-Emitting Diodes: Basic Properties. In *Highly Efficient OLEDs with Phosphorescent Materials*; Wiley-VCH: Weinheim, Germany, 2008; pp 1−97.

(39) Liu, D.; Ren, H.; Deng, L.; Zhang, T. Synthesis and Electrophosphorescence of Iridium Complexes Containing Benzothia-zole-Based Ligands. *ACS Appl. Mater. Interfaces* **2013**, *5*, 4937−4944.

(40) Tong, B.; Mei, Q.; Chen, D.; Lu, M. Synthesis and Electroluminescent Properties of Red Emissive Iridium(III) Complexes with Ester-Substituted Phenylquinoline Ligands. *Synth. Met.* **2012**, *162*, 1701−1706.

(41) Pan, B.; Wang, B.; Wang, Y.; Xu, P.; Wang, L.; Chen, J.; Ma, D. A Simple Carbazole-N-Benzimidazole Bipolar Host Material for Highly Efficient Blue and Single Layer White Phosphorescent Organic Light-Emitting Diodes. *J. Mater. Chem. C* **2014**, *2*, 2466−2469.

(42) Gong, S.; Sun, N.; Luo, J.; Zhong, C.; Ma, D.; Qin, J.; Yang, C. Highly Efficient Simple-Structure Blue and All-Phosphor Warm-White Phosphorescent Organic Light-Emitting Diodes Enabled by Wide-Bandgap Tetraarylsilane-Based Functional Materials. *Adv. Funct. Mater.* **2014**, *24*, 5710−5718.

(43) Gong, S.; Chen, Y.; Luo, J.; Yang, C.; Zhong, C.; Qin, J.; Ma, D. Bipolar Tetraarylsilanes as Universal Hosts for Blue, Green, Orange, and White Electrophosphorescence with High Efficiency and Low Efficiency Roll-Off. *Adv. Funct. Mater.* **2011**, *21*, 1168−1178.

(44) Lai, S. L.; Tong, W. Y.; Kui, S. C.; Chan, M. Y.; Kwok, C. C.; Che, C. M. High Efficiency White Organic Light-Emitting Devices Incorporating Yellow Phosphorescent Platinum(II) Complex and Composite Blue Host. *Adv. Funct. Mater.* **2013**, *23*, 5168−5176.